Non-destructive evaluation of material state by acoustic, electromagnetic and thermal techniques

MATSUMOTO Eiji, and ABE Masataka

Department of Energy Conversion Science, Kyoto University, Kyoto 606-8501 Japan (matumoto@energy.kyoto-u.ac.jp)

Abstract: This paper considers non-destructive evaluation techniques for integrity of structural materials of nuclear power plants. To increase the safety and reliability of long term operating plants, the exact remaining life of each component should be predicted by estimating material states such as the degree of degradation and mechanical states affecting the remaining life. Mechanical fatigue (for instance, degradation and residual stress) and plastic deformation (*e.g.* mechanical states) have been considered. Conventional flaw detection techniques cannot be applied to estimate such material states without the apparent geometrical changes. On the other hand, mechanical, electromagnetic or thermal properties of the material may change by several mechanisms. Several NDE techniques are proposed for the purpose and they are acoustic impedance method using phased array transducer, magnetoacoustoelasticity, magnetic flux leakage testing (MFLT), and thermograph combined with magnetic heating. Feasibility of the proposed techniques is discussed by applying them to typical carbon steel specimens.

Keyword: fatigue; plastic deformation; NDE; acoustic impedance; magnetic properties

1 Introduction

Non-destructive evaluation (NDE) techniques are required in order to ensure long time operation and improve operation rate of nuclear power plants (NPPs). NDE techniques can estimate the integrity of the structural materials with all stages of material degradation. Conventional NDE techniques are effective for detection and sizing of flaws, while they cannot estimate the earlier stage of material degradation before crack initiation. Furthermore, it is known that some mechanical states of the material influence its remaining life. Indeed, residual stress influences crack growth, and plastic deformation suppresses mechanical strength and fatigue life. Degradation and aging of materials used in NPPs were recently summarized by Livingston *et al.* [1] and Andresen *et al.* [2]. The feasibilities of various techniques to assess early material degradation were reviewed by Bond and co-workers [3]. Matsumoto [4] applied new NDE techniques based on measurement of material properties to austenite stainless steel. In this paper several NDE techniques are proposed by using acoustic, electromagnetic and thermal properties of materials and verify the applicability to estimate the various material states. In the next section discussions are made on requirements for specimens suitable to evaluate NDE techniques and measurement mechanisms of the proposed techniques. In sections 3 and 4 applications are made of the techniques to fatigue and plastic deformation with residual stress of carbon steel specimens, respectively. The last section gives the summary of obtained results.

2 NDE using material properties

2.1 Specimens for NDE experiments

To obtain calibration data for qualitative estimation, specimens of the objective material were subjected to several degrees of fatigue, plastic deformation and stress. Stress distribution in the specimen was calculated by FEM analysis for design of shape and determination of applied stress level. In general, specimens for NDE experiments should satisfy several requirements, different from conventional mechanical tests. That is, (R1) the specimens have suitable dimensions sufficiently large for NDE; (R2) for calibration they are subjected to prescribed fatigue degree, plastic deformation or residual stress; (R3) for verification of applicability they have a localized region with fatigue, plastic deformation or residual stress.

2.2 Acoustic impedance method

Received date: August 15, 2012
(Revised date: September 12,2012)

Acoustic impedance is defined as the product of the mass density and the mechanical wave speed. Conventional ultrasonic flaw inspection techniques utilize reflected pulses to obtain the location of reflectors and the strength of their reflections. The received waveform also includes small disturbances reflected from each point of the inhomogeneous region as a convolution. Izumiya *et al*. [5] reported a method to obtain layered inhomogeneity (acoustic impedance) by waveform analysis, and Matsumoto *et al*. [6, 7] proposed an algorithm to obtain two-dimensional inhomogeneity using the aperture synthesis, and applied to estimate the local fatigue and SCC in welded part by constructing a new phased array ultrasonic transducer.

Acoustic impedance of the specimen surface can be obtained in more simple procedure. That is, by calculating the ratio R of the amplitudes of the incident and the reflected pulses at the boundary of two materials, we obtain:

$$\rho_2 c_2 = \frac{1-R}{1+R}\rho_1 c_1 \qquad (1)$$

where ρc is the acoustic impedance, and subscripts 1 and 2 distinguish the incident and the transmitted materials. Using a phased array ultrasonic transducer, we can obtain the linear distribution of the acoustic impedance on the specimen surface. The phased array system used in this paper can store the received waveforms given by all the combinations of 32 elements to computer.

2.3 Magnetoacoustoelasticity

This technique utilizes magnetoelastic coupling, *i.e.*, the interaction between magnetic and mechanical fields in ferromagnetic materials. For example, magnetostriction, stress magnetization effect, and dependences of stress-strain and magnetization curves on magnetic and stress fields, respectively. It is considered that such an interaction is sensitive to the microstructure of the material as well as the applied magnetic and stress fields. The coupling gives rise to magnetoacoustic effect in propagation of elastic waves, which is applied to residual stress evaluation by measuring the speed change of ultrasonic waves by magnetization[8, 9]. It is expected that mechanical fatigue and plastic deformation also affect the magnetoacoustic effect due to microscopic change in metallic structure.

2.4 Magnetic flux leakage testing

New magnetic sensors with high sensitivity can detect the weak magnetic flux leakage generated from magnetic inhomogeneity of ferromagnetic materials. Scanning such a small sensor with high spatial resolution enables to obtain the precise distribution of the leakage flux, which was applied to estimate defect shapes (see Abe *et al*. [10]). When cyclic or large stress is applied to the specimen, the local magnetic permeability and the remanent magnetization will change in stress-concentrated region. In order to apply this method to quantitatively estimate the material state, the correlation of magnetic flux leakage and fatigue degree or plastic strain *etc*. should be obtained.

2.5 Thermograph with magnetic heating

If a specimen with a surface defect is heated by a certain method, the temperature distribution will occur around the defect due to the difference in the heat transfer to air. Such a temperature distribution can be visualized as an infrared image by a thermography, which can be used as a NDE technique of surface defects. If a magnetic field with low frequency is applied to the specimen with defects or magnetic inhomogeneity, the region with larger magnetic flux density or larger magnetic hysteresis will be selectively heated by hysteresis loss of the external magnetic field (see Yamada *et al*. [11]). Infrared images by magnetic heating may be applied to mechanical fatigue, plastic deformation or residual stress if magnetic inhomogeneity is induced by them.

3 NDE of mechanical degradation

3.1 Specimens

Mechanical fatigue of carbon steel STS410 (which is used as structural components of NPPs) was considered. High-cycle fatigue test at several stress levels were performed to obtain SN curve and to determine an appropriate stress level and the corresponding cycle number to failure. To assign the position of crack nucleation, a non-penetrating notch was introduced in the center of each specimen. The results of fatigue test are plotted in Fig.1. The

obtained fatigue lives have large variance when the loading frequency is 20 Hz, which may be caused by increase of specimen temperature. In consideration of this, the frequency in the subsequent cycles was set at 10 Hz. The specimen failed at 297,544 cycles under the nominal stress amplitude 190 MPa. The specimens were then prepared with cumulative fatigue coefficients ranging from 0.1 (10%) to 0.8 (80%) of the fatigue life under the nominal stress amplitude of 190 MPa.

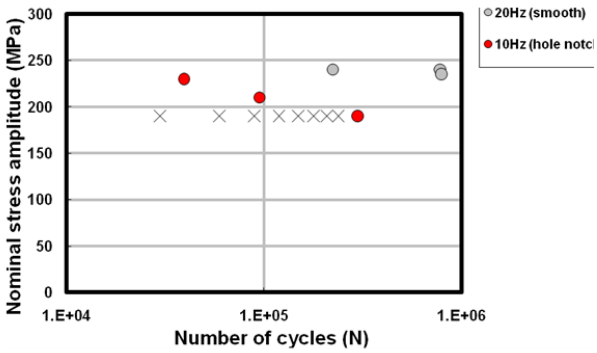

Fig.1 Results of fatigue test for carbon steel STS410.

3.2 Acoustic impedance method

In a logical sense, this technique can obtain the vertical distribution of the acoustic impedance. For the purpose of this paper, however, it is sufficient to measure the acoustic impedance of the specimen surface at each fatigue degree. Fig. 2, which shows the average of the acoustic impedances measured by all elements near the introduced notch at each fatigue degree, indicates that the acoustic impedance decreases with fatigue. Since the acoustic impedance mainly depends on the wave speed, the result reflects the stiffness decrease during cyclic loading. This may be caused by microscopic structural change such as accumulation of dislocations and local stress-induced phase transformation etc., whose analysis is beyond the scope of this paper. Henceforth, the dimension of the acoustic impedance (kg/m^2s) is omitted for simplicity.

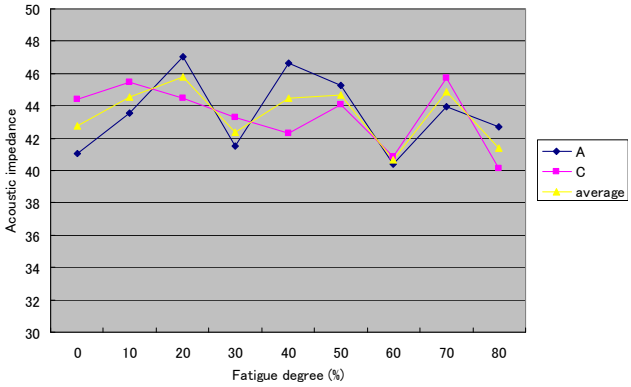

Fig.2 Acoustic impedance at each fatigue degree.

3.3 Magnetoacoustoelasticity

Acoustoelasticity has been applied to residual stress evaluation by measuring the speed change of ultrasonic wave due to mechanical nonlinearity. It is considered, however, that availability of the method is restricted due to difficulty posed in highly accurate measurements of propagation time and distance of the wave. Conversely, magnetoacoustoelasticity utilizes the speed change of an ultrasonic wave by magnetization, which can eliminate main errors in acoustoelasticity. The magnetic field along the specimen axis and transmit ultrasonic waves in the depth direction was applied. In this case three kinds of wave modes may exist, *i.e.*, a longitudinal wave and two transverse waves oscillating in the axial and the width directions of the specimen. The result for the transverse wave oscillating in the parallel direction to the specimen axis is only shown. For simplicity, we define the speed change of the wave by magnetization as 'the magnetoacoustic effect'. Fig. 3 indicates that the magnetoacoustic effect increases with fatigue degree if fluctuation is neglected.

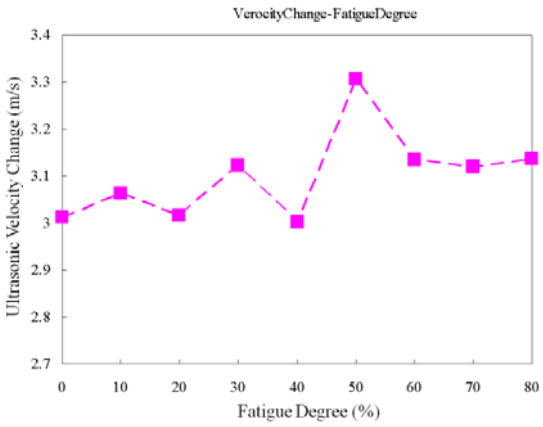

Fig.3 Magnetoacoustic effect at each fatigue degree.

3.4 Magnetic flux leakage testing

After applying the magnetic field along the specimen axis, the inhomogeneous remanent

magnetization may be distributed due to the local fatigued region, which gives rise to the distribution of the magnetic flux leakage. The magnetic sensor in a central rectangular region of the specimen was scanned. Figure 4 shows the maximum value of the tangential (and axial) magnetic leakage flux in the scanning region at each fatigue degree. The flux leakage increases in later fatigue phase, which indicates the increase of the remanent magnetization due to the increase of pinning sites of domain wall movement. The variation of the flux leakage in earlier fatigue phase may arise from the change of domain structure by the magnetoelastic couplings, although its precise mechanism needs further investigation.

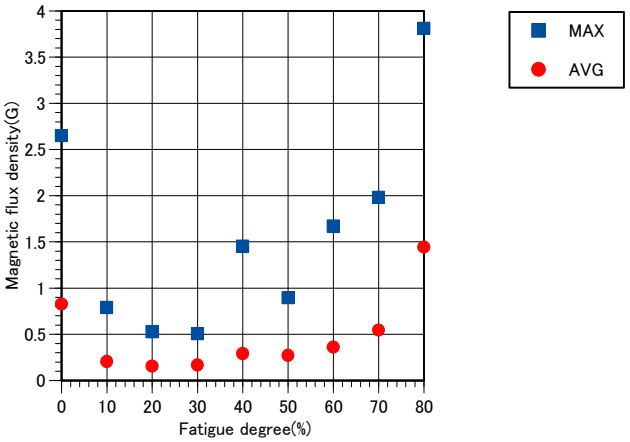

Fig.4 Tangential component of magnetic flux leakage at each fatigue degree.

3.5 Thermograph with magnetic heating

A cyclic magnetic field with 60 Hz frequency was applied for 40 seconds to the specimen at each fatigue degree. The resulting temperature distribution on the specimen surface near the notch during the magnetic heating was measured by the infrared thermography. Figure 5 indicates the increase of the mean temperature near the notch at the end of heating period. It is apparent that the temperature increase becomes larger with fatigue degree. This fact may reflect the increase of the magnetic hysteresis by fatigue. Figure 6 shows the distribution of the temperature increase near the notch at 80% fatigue degree. The temperature increase in the interior of the notch is scaled out to emphasize the one outside the notch. It is clear that small fatigue cracks are developing from both side edges of the notch where the local stress and the local fatigue degree are supposed to be maximum.

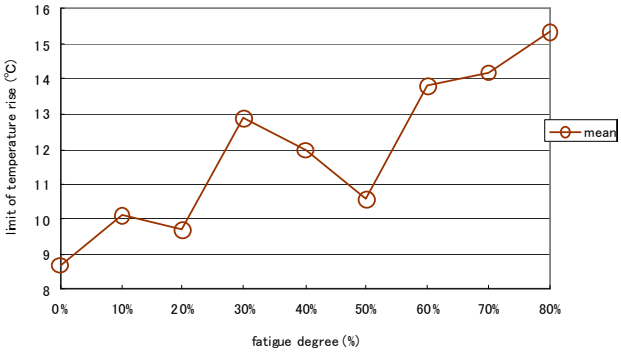

Fig.5 Temperature increase by magnetic heating at each fatigue degree.

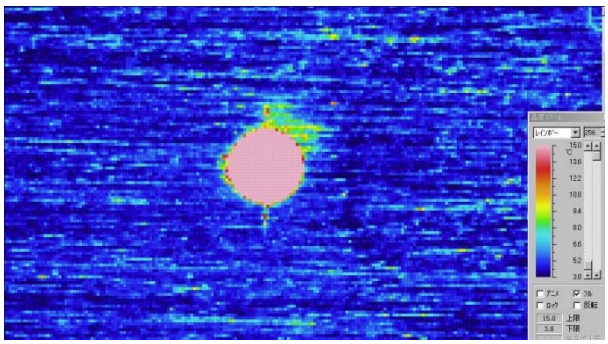

Fig.6 Distribution of temperature by magnetic heating around notch for 80% fatigue degree.

4 NDE of plastic strain and residual stress

4.1 Specimens

Plastic deformation and residual stress of carbon steel SS400 which is commonly used as structural material including NPPs was considered. Three types of specimens for calibration tests in elastic and plastic ranges and for verification of applicability to local deformation were prepared. Prior to preparing specimens tension tests were performed, and obtained the yielding and the fracture stresses, respectively, as 390 MPa and 500 MPa for SS400.

To obtain calibration data for (residual) stress in elastic range, we applied each technique to a single specimen at each stress level in the elastic range. To obtain data for plastic strain, we prepared plastically-

deformed specimens by applying maximum strains 0.0125, 0.0250, 0.0375 and 0.0500, where induced residual (plastic) strains are 0.0111, 0.0232, 0.0353 and 0.0476, respectively. The stress-strain curve in case of 0.0250 maximum strain is shown in Fig.7. For verification of NDE techniques, we prepared two specimens with U-notches on both sides in the center, and applied them the stress to yield maximum strains 0.03 and 0.05 at the stress concentrated position. From the above correspondence between the maximum applied strain and plastic strain, it is expected that local plastic strain is induced in the center region of the specimen. In addition, after removing the applied tension, the plastic tension strain remains in the center region, which induces compressive residual stress in the same region and tensile residual stress outside the region.

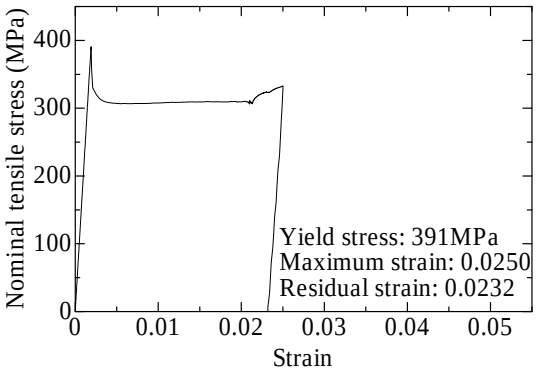

Fig.7 Stress-strain curve of carbon steel SS400.

4.2 Acoustic impedance method

We set the array direction of the phased array system to the specimen axis. Similarly to the case of fatigue, the surface acoustic impedance at the positions of 32 elements was obtained. Since the width of each element and the distance of adjacent elements are small, the distribution of the acoustic impedance fluctuates due to surface roughness or inhomogeneity of the specimen. The average of the surface acoustic impedances measured at each stress level in elastic range is shown in Fig.8. It is clear that the surface acoustic impedance decreases with the elastic stress.

Similarly, the average acoustic impedance of the specimens with plastic strains was obtained. In Fig.9 the horizontal axis denotes the maximum applied strain corresponding to plastic strain as indicated in subsection 4.1. From the figure, we see that the acoustic impedance decreases with the plastic strain. On the other hand, the distribution of the acoustic impedance fluctuated more compared with the elastic range, which may be caused by the increase of surface roughness due to plastic strain. Figure10 shows the linear distribution of the acoustic impedance in the center region of the specimen which was obtained by scanning the phased array system along the specimen axis. Each colored plots denote 32 data measured by the phased array system at each position. According to the increase of surface roughness due to the local plastic strain, the distribution has large fluctuation in the center of the specimen. From such fluctuation of the surface acoustic impedance, qualitative evaluation of plastic strain seems difficult at the present stage. Conversely, such fluctuation of surface acoustic impedance will be effective to detect the plastic region.

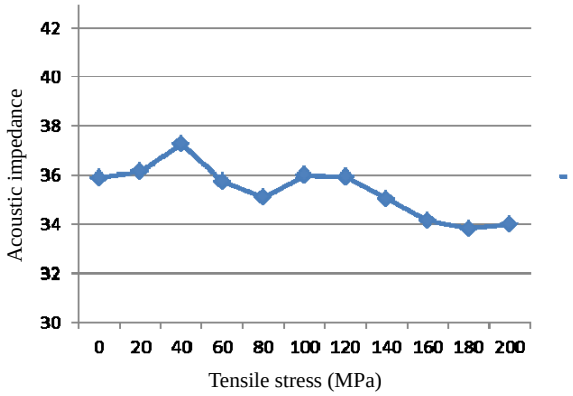

Fig.8 Variation of acoustic impedance by elastic stress.

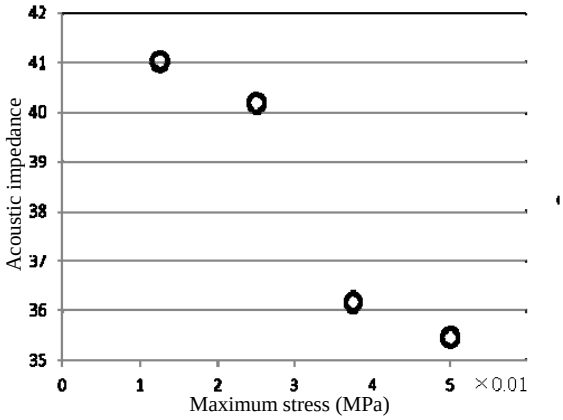

Fig.9 Variation of acoustic impedance by plastic strain.

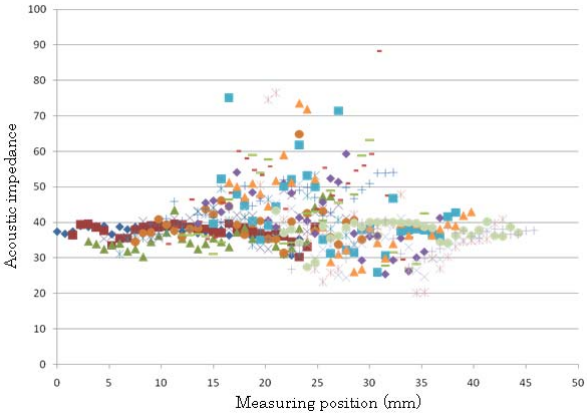

Fig.10 Distribution of acoustic impedance by local plastic strain (0.03 maximum applied strain).

4.3 Magnetoacoustoelasticity

A strong cyclic magnetic field along the axis of the specimen was subjected to each stress in elastic range. The variation of the ultrasonic transverse wave oscillating in normal direction to the specimen axis by magnetization was then measured. For simplicity, the variation of the wave speed is defined as “the magnetoacoustic effect”, where it should be noted that the considered oscillating direction is different from that in subsection 3.3 for fatigue. Figure 11 indicates the variation of the magnetoacoustic effect by the stress in the elastic range, where three curves were obtained by different specimens. It is apparent that the magnetoacoustic effect decreases with the stress, which may be caused by the decrease of the shear stiffness through the magnetoelastic coupling. Figure 12 shows the variation of the magnetoacoustic effect by the plastic strain. It seems that the magnetoacoustic effect decreases with the small plastic strain and tends to be constant for larger plastic strain.

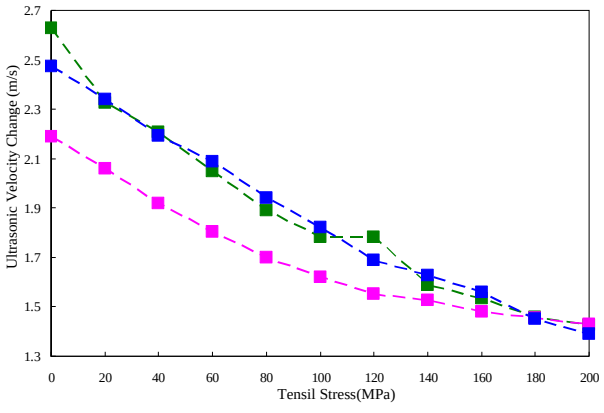

Fig.11 Variation of magnetoacoustic effect by elastic stress.

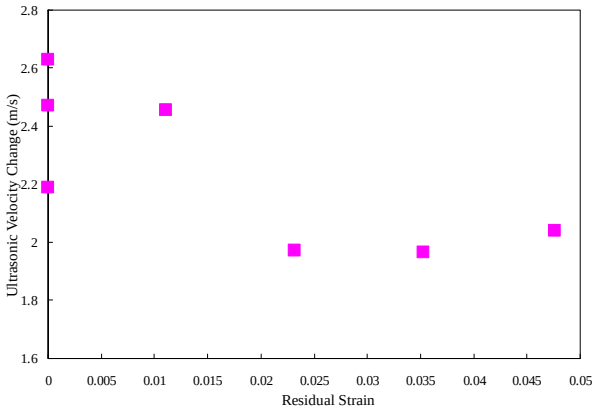

Fig.12 Variation of magnetoacoustic effect by plastic strain.

Figure 13 shows the distribution of the magnetoacoustic effect in the center of the specimen, where the pitch of the measuring points coincides with the diameter of the ultrasonic transducer. The magnetoacoustic effect takes value 1.9 m/s at the center which nearly equals the minimum value corresponding to the residual (plastic) strain around 0.030 in Fig.12. Values 1.4-1.5 m/s of the magnetoacoustic effect at the adjacent points to the center cannot be explained by the plastic strain from Fig.12. On the other hand, in view of Fig.11, we see that the above values of the magnetoacoustic effect are given by tensile stress of 175-200 MPa. This fact implies that the tensile residual stress is induced in the adjacent region of the plastic region.

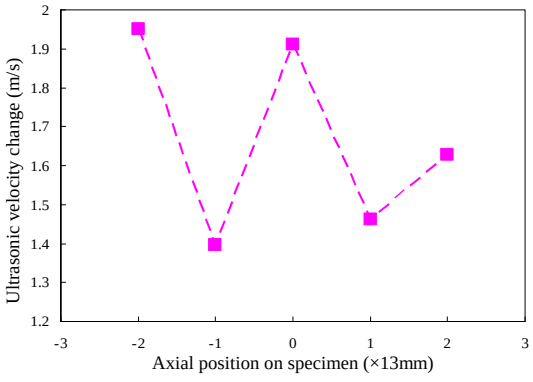

Fig.13 Distribution of magnetoacoustic effect by local plastic deformation (0.05 maximum applied strain).

Conversely a compressive residual stress should be induced in the plastic region, which has the effect of increasing the magnetoacoustic effect from the extrapolation of the curve in Fig.11. Thus, in the central plastic region the opposite magnetoacoustic

effects are superposed, and more information is necessary to decompose them to two contributions due to the plastic strain and the residual stress.

4.4 Magnetic flux leakage testing

Similarly to the case of fatigue, we apply the magnetic field along the specimen axis and measure the tangential (and axial) component of the magnetic flux leakage. The magnetic sensor in a central rectangular region was scanned to obtain the average in the scanning region. Furthermore, weak magnetic flux leakage is measured even for the demagnetized specimen in order to take the difference from the data in the demagnetized state. Figure 14 shows that the obtained magnetic flux leakage decreases in small stress range and tends to increase for larger stress. Such complicated dependence of the magnetoelastic coupling can be seen in some ferromagnetic materials, where we do not delve into the analysis of the phenomenon. Figure 15 shows the variation of the magnetic flux leakage in plastic range, where three plots at each residual strain was obtained for different specimens. If we exclude the two fluctuated plots, apparent dependence of the magnetic flux leakage on the residual strain cannot be seen. It should be noted, however, that by comparing Figs. 14 and 15, the intensity of the magnetic flux leakage in plastic range is rather larger than that of elastic range.

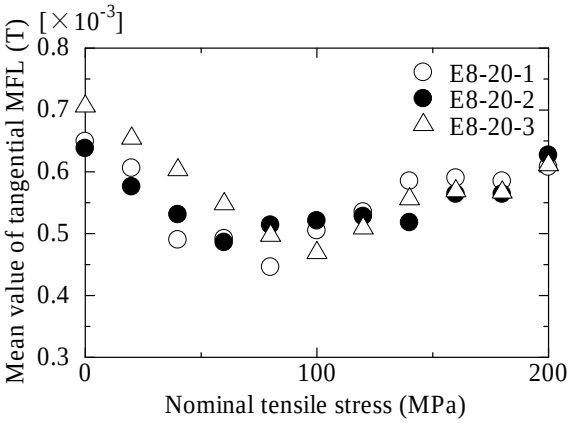

Fig.14 Variation of tangential magnetic flux leakage by elastic stress.

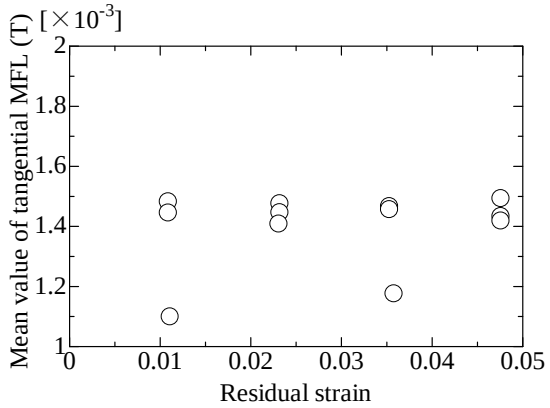

Fig.15 Variation of tangential magnetic flux leakage by plastic strain.

Figure 16 shows the linear distribution of the magnetic flux leakage in the center of the specimen with U-notches on both sides. Specimens D-1, D-2 and D-3 are, respectively, undeformed, and subjected to the maximum applied strains (plastic range) of 0.03 and 0.05. The distribution for D-2 has a plateau with higher leakage in the central of the specimen, which indicates the plastic region. Since the magnetic flux leakage is constant for larger plastic strain in Fig.15, the distribution has a flat region with higher value in the center. Specimen D-3 is subjected to larger stress but the distribution of the magnetic flux leakage exhibits a wider gentle peak differently from the case of D-2. The level of the leakage of D-3 is, however, similar to or larger than the one of D-2, which may imply that the induced plastic region is rather wider than the one of specimen D-2. This idea is supported by the numerical simulation and the difference in the distributions of the acoustic impedance for D-2 and D-3, where the later is omitted.

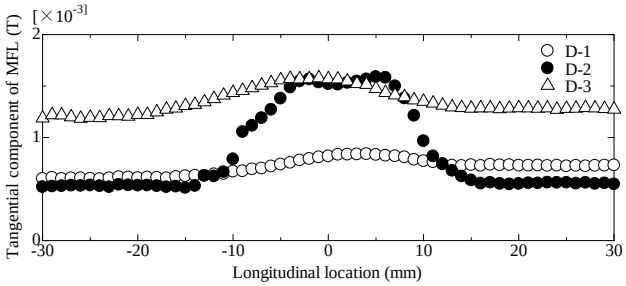

Fig.16 Distribution of tangential magnetic flux leakage near plastic region.

4.5 Thermograph with magnetic heating

In this paper, this technique has not been applied to the specimens described in subsection 4.1. To show the applicability to detection of the plastic region, the variation of the temperature increase in the central region of the specimens subjected to large

deformation as shown in Fig. 17. Here, the horizontal axis denotes the maximum applied stress. From the discussion in subsection 4.1, the applied stress levels is around the yielding stress 390 MPa. Thus, from Fig.17, it is clear that the temperature increase becomes large when the stress is approaching to the yielding point and tends to be constant when the stress exceeds the yielding point. In other words, this phenomenon indicates a transitional change of the magneto-mechanical property of SS400 around the yielding stress. This result is consistent with the plots in Figs. 14 and 15, which show that the magnetic flux leakage increases when the stress exceeds the yielding point and tends to be constant for larger stress in plastic range.

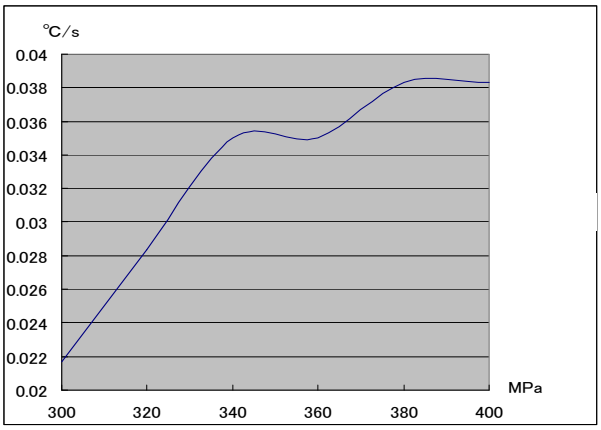

Fig.17 Variation of temperature increase by magnetic heating by stress around yielding point.

5 Conclusion

Acoustic impedance, magnetoacoustic, magnetic flux leakage and thermal techniques were applied to estimate material states such as fatigue degree, elastic stress and plastic strain. Carbon steel specimens suitable for NDE experiments were designed and used to gauge the feasibility of the proposed techniques.

The obtained results in this paper are summarized as follows:

1. It was found that many measured calibration data by four techniques have monotone correlations with the fatigue degree, elastic stress and plastic strain. Such monotone correlations will be useful for qualitative estimation.
2. Acoustic impedance method was applied to obtain the surface distribution, which had a fluctuation due to the inhomogeneity surface conditions. Although the increase of such a fluctuation in plastic region makes qualitative estimation difficult, it enables us to identify the plastic region. This method has a possibility to obtain two dimensional distribution of the material states.
3. Magnetoacoustic effect, *i.e.*, the speed changes of ultrasonic transverse waves by magnetization, has rather apparent correlation with the plastic strain and the stress. Rough estimation of the plastic strain and the residual stress was achieved for a specimen with local plastic region.
4. Variations of the magnetic flux leakage by fatigue, elastic and plastic deformations were complicated, while it is available to identify the plastic region from the distribution of the magnetic flux leakage.
5. Thermal method, *i.e.*, temperature increases by magnetic heating was applied only to fatigued specimen, where the possibility of visualizing the fatigued region was shown.
6. Exact qualitative and local estimation (coexisting case of plastic strain and residual stress) as well as applications to actual components, are left as future topics.

Acknowledgement

NDE of fatigue of this study was performed as Coordinated Research Project by International Atomic Energy Agency, and NDE of plastic deformation as collaborative research with Kansai Electric Power Co., Inc.. The authors would like to express our thanks to all the concerned persons.

References

[1] LIVINGSTON, J.V., CHATTOPADHYAY, S., HOOPINGARNER, K.R., PUGH, E.A., and PACIFIC NORTHWEST LABORATORY: A Review of Information for Managing Aging in Nuclear Power Plants. PNL-10717; Part 2 of 2. Richland, Washington: Pacific Northwest Laboratory, 1995.

[2] ANDRESEN, P.L., FORD, F.P., GOTT, K., JONES, R L., SCOTT, P.M., SHOJI, T., STAEHLE, R.W., and TAPPING, R.L.: Expert Panel Report on Proactive Materials Degradation Assessment, NUREG/CR-6923; BNL-NUREG-77111- 2006, Washington DC: US Nuclear Regulatory Commission, 2006.

[3] BOND, L.J., DOCTOR, S.R., GRIFFIN, J.W., HULL, A.B., and MALIK, S.N.: Damage Assessment Technologies for Prognostics and Proactive Management of Materials Degradation (PMMD), Nuclear Technology: in print; 2011.

[4] MATSUMOTO, E.: Non-Destructive Evaluation of Fatigue by Thermal, Acoustic and Electromagnetic Techniques. In: Proceedings of International Conference on the Mechanical Behaviour of Materials, 2011.

[5] IZUMIYA, T., MATSUMOTO, E., and SHIBATA, T.: Nondestructive Measurement of Inhomogeneity of Functional Gradient Materials by Using Elastic Wave Analysis, Transaction of the Japan Society of Mechanical Engineer, 1995, 61A (59): 2421-2428(in Japanese).

[6] MATSUO, K., MATSUMOTO, E., and BIWA, S.: Evaluation of Inhomogeneity by Phased Array Ultrasonic Transducer. In: Proceedings of the 20th Symposium on Electromagnetics and Dynamics, 2008: 51-54(in Japanese).

[7] EBISUI, D., TATEMATSU, N., and MATSUMOTO, E.: Non-Destructive Evaluation of Fatigue Degree of Metal by Ultrasonic Phased Array System. In: Proceedings of the 19th Conference on Electromagnetic Phenomena and Dynamics, 2010: 261-264 (in Japanese).

[8] MIZOKAMI, M., YUN, K., BIWA, S., and MATSUMOTO, E.: Measurement of Orthotropic Elastic Coefficient of Ferromagnetic Materials Using Ultrasonic Wave Speed and Magnetostriction. In: Proceedings of the 19th Conference on Electromagnetic Phenomena and Dynamics, 2008(in Japanese).

[9] MATUMOTO, E., MIKI, K., and SHIBATA, T.: Measurement of Stress and Magnetization by Ultrasonic Transverse Waves, Journal of Electrical Engineering, 1997, 48(8/S): 46-49.

[10] ABE, M., BIWA, S., and MATSUMOTO, E.: 3D Shape Identification of Parallelepiped Flaw by Means of Biaxial MFLT Using Neural Network, International Journal of Nuclear Safety and Simulation, 2009, 1(1): 63-71.

[11] YAMADA, S., MATSUMOTO, E., and BIWA, S.: Visualization of Surface Defects of Steel Using Iron Loss and Infrared Thermography. In: Proceedings of 5th Annual Conference of the Japan Society of Maintenology, 2008: 231-236.